# Maximum depth of local scour near emerged vertical-wall spur dike

Hossam M. Nagy
*Irrigation Eng. and Hydraulics Dept., Faculty of Eng., Alexandria University, Alexandria, Egypt*

Based on the flow continuity equation, the generalized form of the momentum equation, the bed scour geometry and the Karman-Prandtl logarithmic law for flow resistance, a semi-empirical analysis of clear-water local scour around a spur-dike is presented. The developed expression for maximum scour depth is derived for a single emerged dike obstructing the flow direction. The expression involves various flow, sediment and geometrical properties, which have significant effect on the scour criteria. The influence of the relevant parameters is investigated in the light of wide-ranging data obtained from experimental research in addition to data collected from other previous studies. A group of 193 experimental data on clear-water scour depth is utilized to develop a discrete form for the expression of maximum scour depth through a statistical nonlinear regression analysis. Results of the new developed model are compared with the results of the other previous studies in the light of the assembled data. The presented model results gave much better agreement with observed data more than the previous formulas.

فى هذا البحث تمت معالجة موضوع العمق الأقصى للنحر الموضعى بالقرب من الرؤوس الحجرية البارزة وذلك من خلال مدخل نظرى وتجارب معملية وأيضا تجميع بيانات سابقة وأخيرا عمل دراسة تحليلية رياضية. هذا وقد إعتمد المدخل النظرى على معادلات الجريان التقليدية مثل معادلة الإستمرار ومعادلة كمية الحركة وعلى الأبعاد الهندسية لحفرة النحر وعلى المعادلة اللوغاريتمية للسرعات ومقاومة الجريان. وقد ثبت من المعالجة النظرية أن رقم فرويد هو من أهم العوامل المؤثرة فى إختلاف عمق النحر النسبى. ومن أهم المتغيرات التى تم دراستها معمليا ومعرفة مدى تأثيرها على عمق النحر النسبى هو الطول النسبى للرأس الحجرى ونسبة الإعتراض والقطر النسبى لحبيبات الرمل وزاوية الميل للرأس الحجرى على المسقط الأفقى. وقد تم إستنتاج معادلة رياضية لحساب عمق النحر الأقصى باستخدام طريقة التحليل الإرتدادى وتمت مقارنتها بالمعادلات السابقة وذلك بالإستعانة بالبيانات المعملية المقاسة والبيانات التى تم تجميعها من أبحاث سابقة. وقد ثبت أن المعادلة الجديدة تفوق مثيلاتها فى دقة الإستنتاج لعمق النحر الأقصى.

**Keywords:** River training, Sediment transport, Clear-water scour, Spur-dikes, Abutments

## 1. Introduction

Many groins or spur dikes have been constructed for training the stream along a desired course by attracting, deflecting or repelling the flow; to protect bank from erosion at high water depth or flood by keeping the flow away from it; and to contract a wide river channel for improving the depth for navigation at low water depth. They also have been used to enhance aquatic habitats by forming stable pools in disturbed streams.

Studies have shown that the local scour phenomena at spur dikes and abutments are quit similar, in which dikes can be viewed as very thin rectangular vertical wall abutments. Local scour is mainly caused by increased flow velocity, local vortices, turbulence and shear intensity near abutments and dikes perpendicular to stream flow. The flow field around a spur dike is generally characterized by acceleration from upstream to the most contracted cross section near the nose of the dike. Downstream of the dike, the main flow is separated from large eddies by a vortex boundary. Far downstream of the reattachment point, uniform flow will be re-established. It is sufficient herein to state that the obstruction caused by the dike generates a complicated system of vortices, which are believed to be the main cause of erosion. The primary horseshoe vortex impinges on the sand bed immediately in front of the spur and throws up the eroded material, which is transported downstream by the main flow. Consequently, the scour hole is developed around the dike. The deepest point of scour is located close to the tip of the dike.

Early studies for local scour near dikes and abutments may be represented herein by the contributions of Ahmed [1], Liu et al. [2], Garde et al. [3], Laursen [4], and Gill [5] among others. Recent studies include Rajaratnam and Nwachukwu [6] and Melville [7]. The studies of Melville [7] & [8] summarized several research studies completed since the beginning of the 1980s at Auckland University.

The subject of prediction of maximum scour depth had the attention of many investigators from several decades till now. There are basically three types of scour-depth prediction approaches in the literature: (i) the regime approach, Ahmed [1], which relates the scour depth to the increased discharge intensity or flow at the abutment location; (ii) dimensional analysis approach (Liu et al. [2], Garde et al. [3], and Melville [7]), where relevant dimensionless parameters describing the phenomenon are correlated; and (iii) analytical or semi-empirical approach, such as those proposed by Laursen [4] and Gill [5], based on a sediment-transport relation for the approaching flow, or based on similarity principle such as those proposed by Oliveto and Hager [9].

In the present study, analytical and experimental analyses are conducted. The scour and flow structure around a single dike is investigated. A semi-empirical expression has been presented to estimate the maximum scour depth. Laboratory experiments under controlled conditions are performed for a uniform size of sediments. A data mining for maximum scour depth problem is carried out from several previous reliable studies related to scour near vertical wall spur dikes and abutments under clear water conditions. A parametric analysis is accomplished to explore the most pertinent parameters for local scour criteria. The effect dike alignment is clarified. A new formula for maximum scour depth is obtained and compared with other previous expressions in the light of the collected data. The results of the new developed expression agreed well with the observed data.

## 2. Theoretical approach

The obstruction caused by the dike generates a complicated system of vortices, which are believed to be the main cause of erosion. The primary horseshoe vortex impinges on the sand bed immediately in front of the spur and throws up the eroded material, which is transported downstream by the main flow. While any analysis of scour phenomenon which takes into account the three dimensional erosive characteristics of the horseshoe vortex will necessarily be complicated, it was found that the equilibrium scour depths could be satisfactorily described by a simple hydrodynamic model.

The flow structure in the region of a single spur dike over a scour hole in equilibrium state is simplified for the purpose of establishing an analytical approach for estimating maximum local scour depth. The velocity profile $u(y)$ in the approaching flow before reaching the location of spur dike is assumed to satisfy the Karman-Prandtl logarithmic law (Rajaratnam and Nwachukwu [6]).

In the region of scour hole, the velocity at any point on vertical cross-section may be represented by:

$$u = u_b + u_s' \, f_1(\zeta, \upsilon), \tag{1}$$

where:

$$\zeta = 1 - \frac{y}{h}, \upsilon = 1 - \frac{z}{b}, u_s' = u_s - u_b \;\; h = h_0 f_2(\upsilon),$$

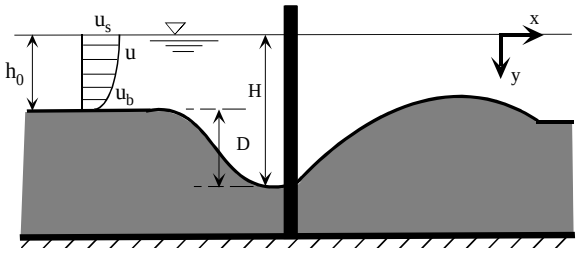


Fig. 1-a. Section (1-1).

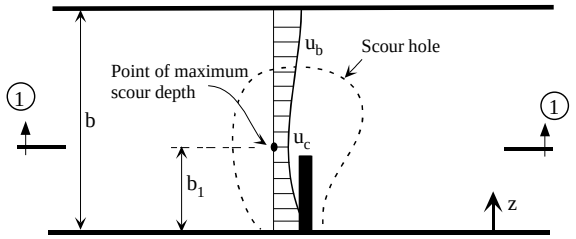


Fig. 1-b. Schematic plan showing the scour hole around a dike.

and $u_b = u_c f_3(\upsilon)$, in which $y$ is the depth from the water surface level, $h$ is the water depth at any point, $z$ is the distance from the side wall, $b$ is the channel width, $u_s$ is the surface velocity, $u_b$ is the bottom velocity, $h_0$ is the flow depth in the approach channel cross section, and $u_c$ is the bottom velocity at point $c$ (the point of maximum depth), as shown in figs 1-a and 1-b.

Applying the continuity equation between two sections; one in the approaching canal and the other over the scour hole, and neglecting head losses through the channel yields:

$$u_0 h_0 b = \int\int_R u dy dz , \quad (2)$$

where $u_0$ is the flow average velocity in the approaching canal. The right hand side of eq. (2) yields:

$$\int\int_R u dy dz = \int_0^{b_1}\int_0^{h} u dy dz + \int_{b_1}^{b}\int_0^{h} u dy dz , \quad (3)$$

in which $b_1$ is the distance between the deepest point of scour hole and the side wall. Normalizing eq. (3) yields:

$$\int\int_R u dy dz = b_1 \int_0^1 h \int_0^1 u d\zeta d\upsilon + (b - b_1) \int_0^1 h \int_0^1 u d\zeta d\upsilon . \quad (4)$$

Substituting terms of eq. (1) into eq (4) and rearranging parameters gives:

$$u_s' = \frac{u_0 - u_c \Omega_1}{\Omega_2} , \quad (5)$$

in which,

$$\Omega_1 = \int_0^1 f_2(\upsilon) f_3(\upsilon) d\upsilon , \Omega_2 = \int_0^1 f_2(\upsilon) d\upsilon \int_0^1 f_1(\zeta, \upsilon) d\zeta \, d\upsilon .$$

Applying the momentum equation between the same two sections:

$$\rho\beta\, u_0^2 h_0 - \rho \int_0^b \int_0^h u^2 dy dz = \rho g\, h_{cg} \int_0^b \int_0^h dy dz - \frac{1}{2} \rho g h_0^2 b , \quad (6)$$

in which, $\rho$ is the flow density, $\beta$ is the momentum correction coefficient, g is the gravitational acceleration, $h_{cg} = H \cdot f_4(\zeta)$ is the distance of the centric point of the respective water area, in which $H$ is the maximum water depth over the scour hole. Solving the two equations and rearranging the resulting terms yield:

$$\frac{H}{h_0} = \left(1 + 2\beta \frac{u_0^2}{g h_0}\right) - 2\varpi_1 \frac{u_c^2}{g h_0} - 4 \frac{u_c}{\sqrt{g h_0}} \frac{u_0}{\sqrt{g h_0}} + 4\varpi_2 \frac{u_c^2}{g h_0} - 2\varpi_3 \frac{u_0^2}{g h_0} + 4\varpi_4 \frac{u_0}{\sqrt{g h_0}} \frac{u_c}{\sqrt{g h_0}} - 2\varpi_5 \frac{u_c^2}{g h_0} , \quad (7)$$

where

$$\varpi_1 = \int_0^1 f_2(\upsilon) f_3{}^2(\upsilon) d\upsilon , \quad \varpi_2 = \int_0^1 f_2(\upsilon) f_3(\upsilon) d\upsilon ,$$

$$\varpi_3 = \frac{\int_0^1 f_2(\upsilon) d\upsilon \int_0^1 f_1^2(\zeta, \upsilon) d\zeta d\upsilon}{\left(\int_0^1 f_2(\upsilon) d\upsilon \int_0^1 (\zeta, \upsilon) d\zeta d\upsilon\right)^2} ,$$

$$\varpi_4 = \varpi_3 \int_0^1 f_2(\upsilon) f_3(\upsilon) d\upsilon , \varpi_5 = \varpi_3 \left(\int_0^1 f_2(\upsilon) f_3(\upsilon) d\upsilon\right)^2 ,$$

and $\varpi_6 = f_4(\zeta) \int_0^1 f_2(\upsilon) d\upsilon$.

For equilibrium condition in the scour hole, the bottom velocity at point c is assumed to be critical for sediment movement. Yang [10] assumed the bottom critical velocity $u_c = 2.05\,\omega$ for shear velocity Reynolds number $u_* d_{50} / \nu$ larger than 70, i.e for rough boundaries, where $\omega$ is the particle fall

velocity, $d_{50}$ is the particle diameter, $u_*$ is the bottom shear velocity and $\nu$ is the kinematic viscosity. Thus:

$$\frac{H}{h_0} = 1 + \varpi_7 F_n^2 \left( 1 + \frac{\varpi_8}{\varpi_7} \left( \frac{F_\omega}{F_n} \right) + \frac{\varpi_9}{\varpi_7} \left( \frac{F_\omega}{F_n} \right)^2 \right), \quad (8)$$

where: $\varpi_7 = 2(\beta - \varpi_3)$, $\varpi_8 = 4(\varpi_4 - 1)$, and $\varpi_9 = 2(2\varpi_2 - \varpi_1 - \varpi_5)$.

The parameter $F_n = u_0 / \sqrt{g h_0}$ is the flow Froude number and $F_\omega = \omega / \sqrt{g h_0}$ is the particle fall velocity Froude number. The fall velocity value is relatively small compared to the flow velocity, and the terms, which contain $F_\omega$ can be neglected without fear of accuracy. Thus, eq. (8) may be simplified into:

$$\frac{H}{h_0} = 1 + \omega_7 \cdot F_n{}^2 . \quad (9)$$

The arameter $\varpi_7 = f(d_{50}/h_0, L/b, L/h_0, \alpha)$, in which $L$ is the dike length, $\alpha$ is the projection angle, and $L/b$ is the intrusion length ratio, $L/h_0$ is the dike length to water depth ratio. Since $H = h_0 + D$, where $D$ is the maximum scour depth measured from bed level, eq. (9) can be simplified as:

$$\frac{D}{h_0} = \omega_7 \cdot F_n{}^2 . \quad (10)$$

The analysis proved that the Froude number, which gives the extent of the influence of gravitational action on flow, is a dominant parameter for scour criteria around spur-dikes. The effect of the other parameters can be illustrated through the statistical analysis of the experimental data.

## 3. Experimental arrangement

Experiments were conducted in a straight tilting plexiglass walled flume with 20 m length, 0.4 m width and having depth of 0.5 m in the Hydraulics Laboratory, Saga University, Japan. The flume has an adjustable slope, $I$. The water was supplied from the underlying sump through re-circulating system. The water then passed through an approach tank provided with a series of baffles. These baffles distributed the flow uniformly over the entire width of the flume and also helped in destroying the excess energy of the flow. The sand bed had a thickness of 20 cm. The sand used in the experiments reported herein has mean size of $d_{50}$ = 0.1291 mm and standard deviation of $\sigma$ = 1.259. The dike models used in the study were made of vertical teakwood planks of thickness 30 mm and projection length of 10 cm. The spur dike nose was rounded. The spur dike was positioned with different angles of inclination of $\alpha$ = 30°, 60°, and 90°, as shown in fig. 2. The sand bed was sited from distance of 5.0 m upstream to 5.0 m downstream of the axis of the spur dike. Before beginning of each run the sand bed was leveled to give the predefined slope. Passing a specific discharge, a constant water level was maintained by adjusting two flip and sliding gates at the tail end. The passing discharge was controlled by using automatic valve located in the supply pipeline. The valve is connected with electronic digital regulator to pass a certain discharge regardless the unsteady pumping supply. Water depth, $h_0$, was measured by using point-gauge mounted on a wooden frame. Velocity measurements were obtained by using two devices; the first is two-dimensional Elector-magnetic current meter consisting of a 7 mm-diameter transducer probe with cable and a signal processor, the second is a propeller current-meter with 3 mm probe diameter. Bed levels along the flume were measured after getting equilibrium state (60 hours) by using bed profile indicator connected with a digitizer. Details of experimental conditions and of the experimental runs are given in table 1, and the scour hole shape is shown in fig. 3.

## 4. Velocity distribution pattern

In all experiments, velocity measurements were taken in vertical plane for several locations. The vertical velocity profiles along

Table 1
Experimental conditions

| Index | Series | $d_{50}/h_0$ | $I$ | $\alpha^0$ | $F_n$ | $D/h_0$ |
|---|---|---|---|---|---|---|
| A3 | NS-11 | 0.0215 | 1/1195 | 90 | 0.37 | 1.92 |
| A4 | NS-12 | 0.0143 | 1/1195 | 90 | 0.27 | 1.11 |
| A5 | NS-13 | 0.0215 | 1/1195 | 60 | 0.37 | 1.63 |
| A6 | NS-14 | 0.0143 | 1/1195 | 60 | 0.27 | 0.98 |
| A7 | NS-15 | 0.0099 | 1/1195 | 60 | 0.24 | 0.77 |
| A13 | NS-16 | 0.0215 | 1/1195 | 30 | 0.37 | 0.83 |
| A14 | NS-17 | 0.0143 | 1/1195 | 30 | 0.27 | 0.28 |
| B3 | NS-01 | 0.0215 | 1/1450 | 90 | 0.37 | 1.75 |
| B4 | NS-02 | 0.0129 | 1/1450 | 90 | 0.23 | 0.75 |

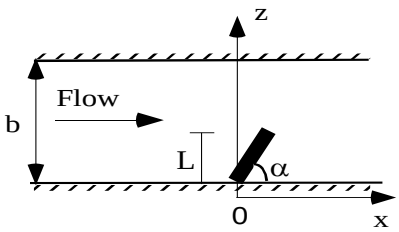


Fig. 2. Schematic plan for angled dike.

Fig. 3. View of final phase of scour hole around dike.

the canal center line were obtained in five locations; one in the approaching flow region, three over the scour hole part, and one over the downstream bed form. In fig. 4, the vertical velocity profiles were plotted to reveal whether they satisfy the Karman-Prandtl logarithmic equation. It was found that for the approaching flow and the flow over the point of maximum scour depth, the velocity data agreed reasonably well with the logarithmic equation. In the downstream part of spur dike the bottom velocity seems to be reversed in direction due to the existence of eddies and vortices.

### *4.1. Bed topography pattern*

In the experiments, different flow conditions and different angles of inclination for dikes are examined. figs. 5-a and 5-b show two graphs representing the topography of bed evolution representing scour hole around dike and downstream sand bars for two angles of inclination, 90° and 30°, respectively. The pair of graphs has similar flow conditions, dike geometry, soil properties. From the graphs it is concluded that the maximum depth of scour is often falls in the upstream side of the structure. Also, it can be demonstrated that attracting spur dike, fig. 5-b, has relatively less scour depth, scour volume, smaller downstream sand waves, and limited effect on the bed near the other side of the channel rather than deflecting spur dike, fig. 5-a.

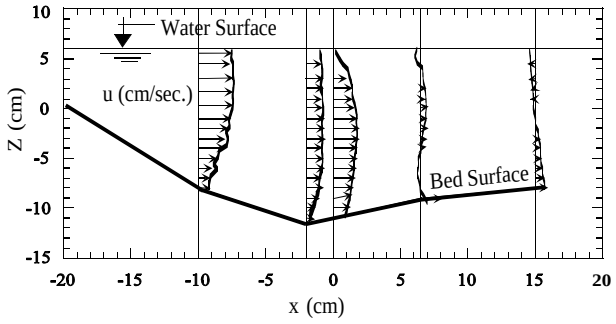


Fig. 4. Velocity distribution along the canal center plane– Run [NS-01].

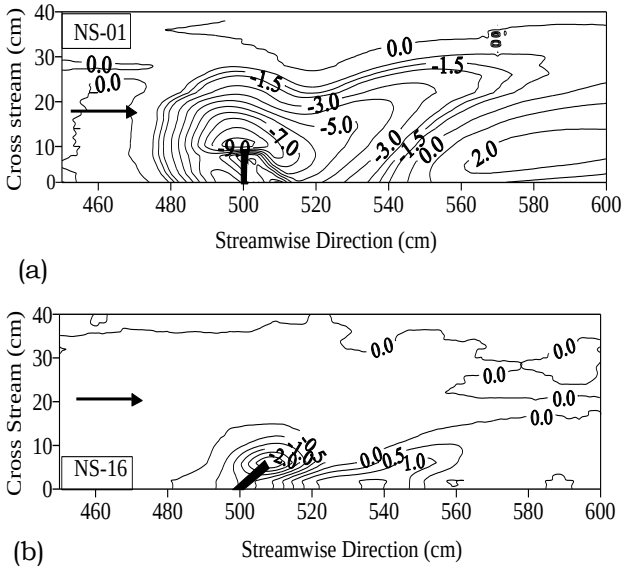


Fig. 5. Topographical maps for scour holes emerged spur dikes for the cases: (a) Dikes with 90° angle of inclination (b) Dikes with 30° angle of inclination.

## 5. Development of maximum scour depth formula

Being able to estimate the maximum scour depth for a given set of boundary conditions is valuable to the design of spur dikes and evaluation of potential effects on the aquatic habitat. The theoretical analysis presented above elucidates the importance of the Froude number as a dominant parameter in the local scour criteria around spur dikes. The effect of other relevant parameters is investigated experimentally. The most pertinent variables affecting such criteria may be presented in the following expression:

$$\frac{D}{h_0} = f\left(d_{50}/h_0,\ L/b,\ L/h_0, \alpha\right) F_n{}^2 . \qquad (11)$$

For predicting the maximum scour depth, it is necessary to formulate this relationship with respect to the presented experimental data and other data collected by the writer from other reliable sources.

## 6. Mining of local scour experimental data

A database of 182 laboratory experiments conducted under clear water scour conditions in rectangular flumes for vertical wall spur dikes has been assembled, analyzed and added to the present measured data. The purposes are to perform a parametric analysis for a wide range of variables and conditions, and to develop a general formula for maximum local scour depth near vertical wall abutments and spur dikes. The data are compiled from the studies of Garde et al. [3], Gill [5], Rajaratnam et al. [6], Zaghlol [11], Kwan [12], Tey [13], Lim [14], and Mamdouh [15]. Table 2 shows the summary of the established database. The data ranges for each of the pertinent parameters are $0.05 \le F_n \le 0.75$, $0.08 \le L/b \le 0.68$, $0.32 \le L/h_0 \le 17.4$, $0.002 \le d_{50}/h_0 \le 0.08$, $0.00003 \le I \le 0.00295$, $1.15 \le \sigma \le 2.2$, $30^0 \le \alpha^0 \le 150^0$. Table 2 shows the range of parameters for the previous studies.

Table 2
Summary of the assembled experimental data for local scour

| Researcher | $d_{50}$ | $\sigma$ | $F_n$ | $L/b$ | $L/h_0$ | $d_{50}/h_0$ | $\alpha$ | Exp. time | No. of points |
|---|---|---|---|---|---|---|---|---|---|
| | mm | | | | | | degree | hrs | |
| Garde [3] | 0.029 | 1.66 | 0.11~ 0.37 | 0.16 | 0.56~2.79 | 0.002~0.08 | 90 | 5 | 18 |
| Garde [3] | 0.10 | 1.38 | 0.34~ 0.39 | 0.08~0.41 | 0.51~2.54 | 0.01 ~0.011 | 90 | 5 | 5 |
| Gill [5] | 0.15 | 1.15 | 0.24~ 0.75 | 0.27 | 2.09~7.79 | 0.015~0.047 | 90 | 6 | 33 |
| Gill [5] | 0.091 | 1.22 | 0.24~ 0.58 | 0.13~0.40 | 1.73~7.30 | 0.016~0.028 | 90 | 6 | 27 |
| Rajaratnam [6] | 0.14 | 1.30 | 0.17~ 0.31 | 0.17 | 0.99~1.42 | 0.009~0.013 | 90 | 166~600 | 6 |
| Zaghlol [11] | 0.45 | 1.30 | 0.18~ 0.40 | 0.33 | 0.47~1.30 | 0.014~0.039 | 90 | 2.5 | 12 |
| Kwan [12] | 0.085 | 1.28 | 0.31~ 0.38 | 0.13~0.68 | 3.28~17.4 | 0.017 | 45~135 | 22 ~ 100 | 11 |
| Tey [13] | 0.082 | 1.26 | 0.25~ 0.38 | 0.11~0.20 | 1.65~6.04 | 0.005~0.016 | 90 | 67 ~ 121 | 4 |
| Siow-Yong Lim [14] | 0.094 | 1.25 | 0.15~ 0.27 | 0.08~0.25 | 0.33~1.00 | 0.006 | 90 | 72 ~ 193 | 11 |
| Mamdouh [15] | 0.051 | 2.2 | 0.05~ 0.24 | 0.10~0.50 | 0.32~2.38 | 0.003~0.006 | 30~150 | 5 | 55 |

## 7. Effect of dike length on the maximum scour depth

The data plotted in fig. 6 shows the effect of intrusion length ratio on the maximum scour depth through a relationship between Froude number and scour depth ratio. Fig. 7 shows the same relation with the parameter, $L/h_0$ representing the dike length related to water depth. It is apparent from both graphs that the scour depth increases with the increase of both intrusion length ratio and dike length to water depth ratio.

## 8. Effect of grain size on the maximum scour depth

Fig. 8 shows the relation between the Froude number and the relative scour depth for different values of sediment grain size. It is clear from the graph that, for the same Foroude number, smaller sediment size yields deeper scour hole. It can be revealed as smaller sediment particles in the scour hole, comparing with larger particles, reach their critical condition of no motion at lower value of critical bottom velocity and lower value of shear stress, which are associated with deeper water depth inside the hole.

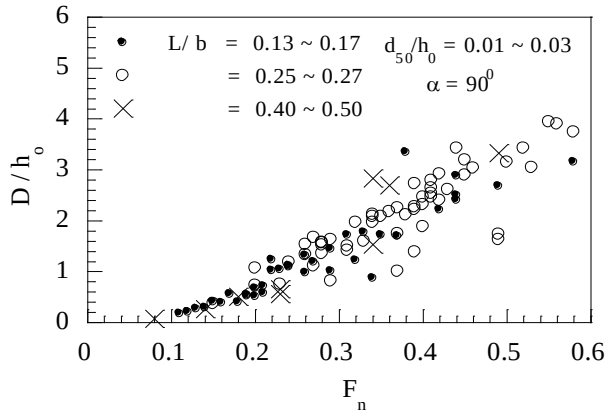


Fig. 6. Effect of intrusion ratio on scour depth.

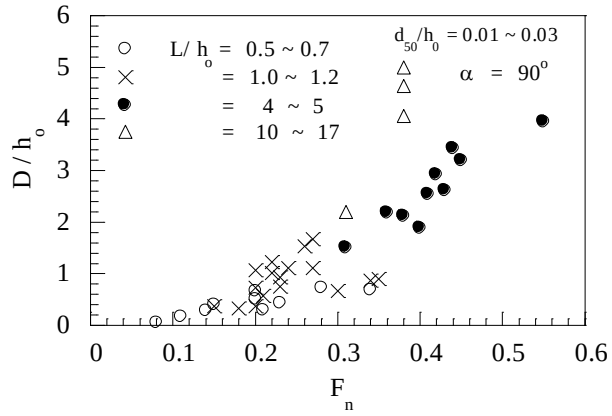


Fig. 7. Effect of dike length ratio on scour depth.

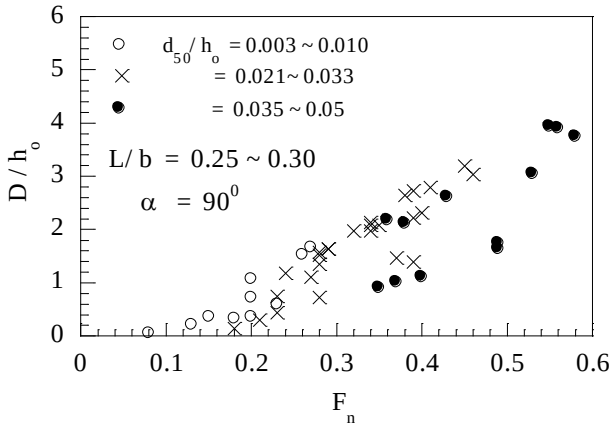


Fig. 8. Dependence of maximum scour depth on particle size.

## 9. Effect of dike alignment on the maximum scour depth

To study the effect of dike alignment on the maximum scour depth, the tabulated experimental data, table 1, in addition to the group of data collected from several reliable sources, table 2, are utilized. Fig. 9 shows a relation between the approaching flow Froude number and the maximum scour depth ratio $D/h_o$ with the parameter $\alpha$ referred to the dike angle of inclination for emerged type of dikes. Five angles of inclination; 30°, 60°, 90°, 120°, and 150° are presented, respectively. Fig. 10 shows the relation between the angle of inclination $\alpha$ and the ratio of maximum scour depth to the maximum scour depth of the dike with 90° angle of inclination, $D_\alpha / D_{90}$. The tested group of data represents all dike lengths; long dikes ($L/h_o > 3$), intermediate dikes ($1 < L/h_o < 3$), and short dikes ($L/h_o < 1$). From the figures, it is concluded that:

1. The maximum scour depth increases with the increase of Froude number for all cases.

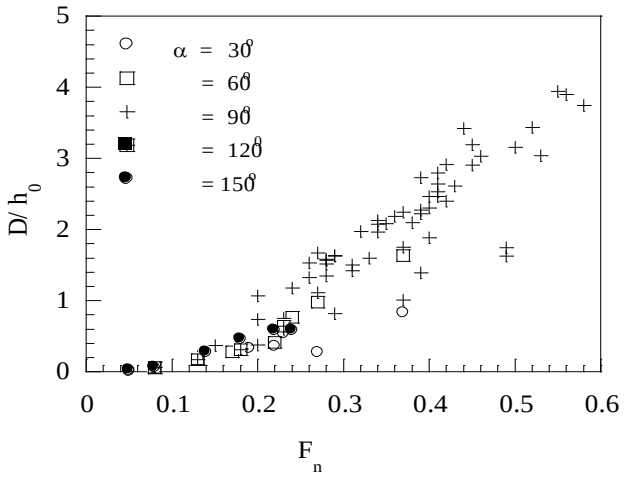


Fig. 9. Relation between $F_n$ and scour depth ratio.

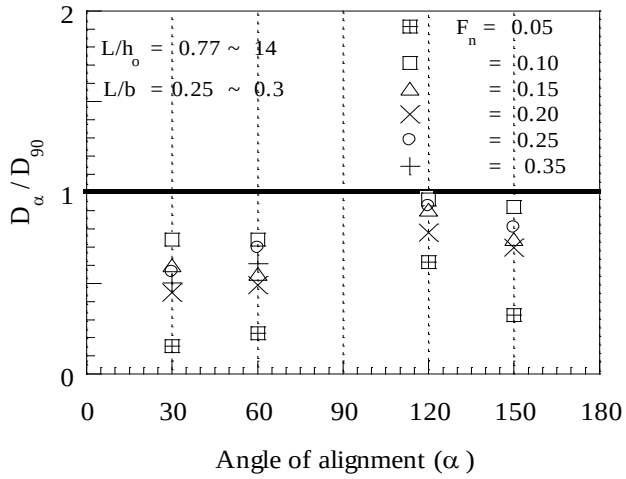


Fig. 10. Effect of $\alpha$ on scour depth.

2. Dikes perpendicular to the bank of the channel cause deeper scour depths more than the attracting dikes (dikes with acute angle with the downstream) or repelling dikes (dike with obtuse angle with the downstream).
3. The dike with inclination angle $\alpha$ < 90° produced the bare minimum scour depth relative to the other two types.

## 10. Froude number-based predictor for maximum scour depth

A multi-regression analysis is applied on the assembled group of data sets which represents a wide range of relevant parameters. The group of data is ranged as shown in table 3. Eq. (11) represents the general form of the expression which contains the relevant parameters for maximum scour depth calculations.

Several algorithms for regression analysis have been examined. The results of such analysis provided a mounting evidence that the dike length ratio, $L/h_0$, has significant effect rather than the intrusion length ratio, $L/b$. The following equation gives the best results for estimating the maximum scour depth ratio, $D/h_0$.

$$\frac{D}{h_0} = 3.0 \quad \frac{(L/h_0)^{0.42}(\sin\alpha)^{0.717}}{(d_{50}/h_0)^{0.277}} \quad F_n^2 . \qquad (12)$$

Fig. 11 shows the line of perfect agreement between measured and calculated maximum scour depth for the 193 data sets which were used in estimating the formula. The mean error is 0.137 and the average standard error is 0.058. Almost 80 % of the data points within the $\pm 50\%$ limit lines. The deviation, between some measured data and the predicted values, is probably due to the difference of experimental time for each research, as shown in table 2.

## 11. Comparison with previous studies

Various ideas and expressions have been proposed by researchers for estimating the maximum local scour depth near abutments and spur dikes in alluvial channels. It is thought necessary to evaluate the new developed expression among the other's previous ones in the light of the collected data.

Table 3
Range of data used for regression analysis

| Parameter | Range |
|---|---|
| $F_n$ | 0.05 ~ 0.75 |
| $L/h_0$ | 0.32 ~ 17.4 |
| $L/b$ | 0.07 ~ 0.68 |
| $d_{50}/h_0$ | 0.002 ~ 0.08 |
| $D/h_0$ | 0.022 ~ 5 |

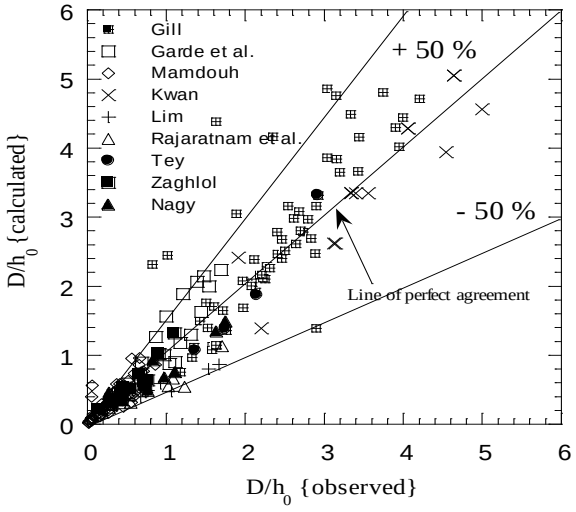


Fig. 11. Comparison between observed and estimated maximum scour depth.

Fig. 12 shows the agreement between observed and predicted data by the expression of Garde et al. [3]. Around 57 % of the data points within the ±50% limit lines, while Gill's [5] Expression in fig.13 gave 50 % only. The Garde et al. [3] equation contains only two parameters; the Froude number and intrusion length ratio. Neglecting the effect of particle size parameter, affects on the accuracy of results, especially for the data of Zaghlol [11],which have large size of particles. The expression presented by Gill [5] gives low accuracy because it doesn't contain the Froude number which represents the most important parameter for scour criteria.

In fig. 14, the data plot shows that the equation of Zaghlol [11] gave underestimated values for all points except of his experimental data. Only 21% of the plotted data located within the ±50% limit lines. In fact, only his data points are fit with his expression because his experimental time is too short comparable with others, see table 2, and the effect of particle size is not included in the expression. Melville [8] presented his integrated expression for all types of dike; however when it is applied specifically for the vertical wall spur dikes, the ratio of 50% of the whole data points located within the ±50% limit lines, as shown in fig. 15. Even he added several coefficients to represent many variables in his integrated formula, the effects of the Froude

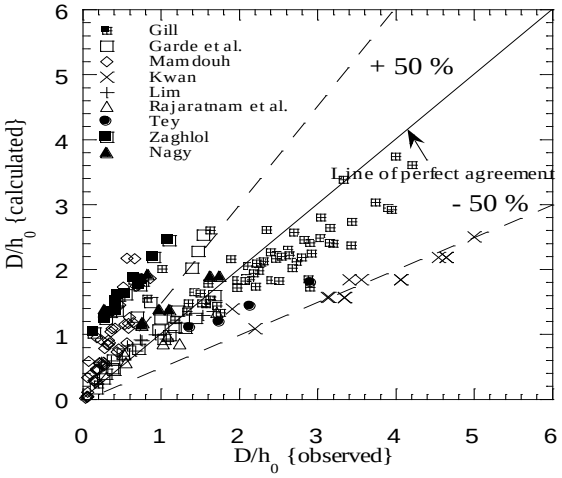


Fig. 12. Verification of Garde et al. [3] equation.

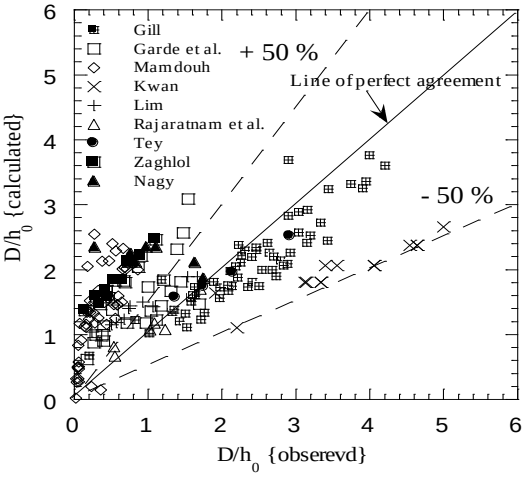


Fig. 13. Verification of Gill [5] equation.

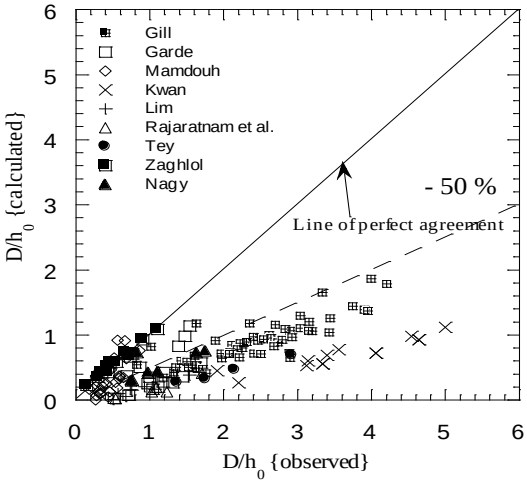


Fig. 14. Verification of Zaghlol [11] equation.

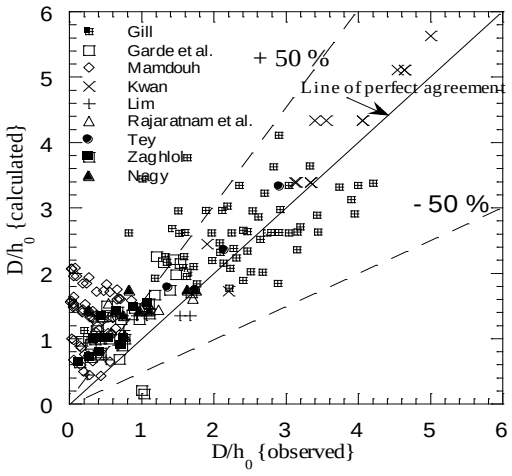


Fig. 15. Verification of Melville. [8 ] equation.

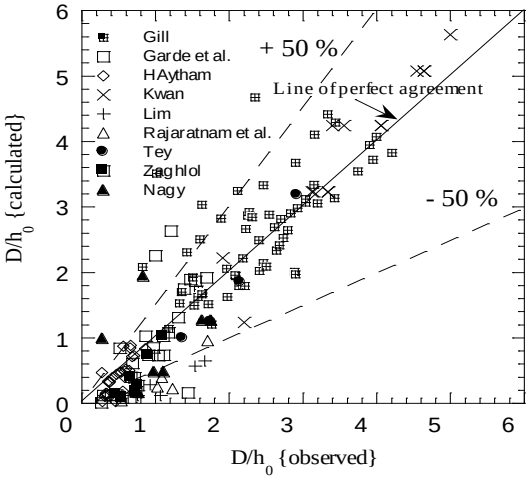


Fig. 16. Verification of Lim [14] equation.

number and particle size were not clarified.

Similarly Lim's [14] expression achieved a ratio of 55 % of the data within the $\pm 50\%$ limit lines, as shown in fig. 16. Only the dike length to water depth ratio was considered a parameter in his equation. The verification of Kandsamy and Melville [16] expression is shown in fig. 17. The ratio of 63% of the whole data points located within the $\pm 50\%$ limit lines. In their expression, they neglected the effect of Froude number, particle size, and angle of dike inclination. Even their equation gave rather better results than others, but it depends mainly on the empirical fitting of data.

It is concluded herein from the above discussion that the results of the presented model, fig. 11, shows better agreement with observed data than the prescribed expressions in this paragraph. The developed formula, eq. 12, has a wide range of application since it has a theoretical base and contains several effective parameters. The scatter of some points may refer to the variation of experimental time for each investigator. It is recommended for future work to define the time limit for experiments to reach the exact equilibrium state of scour.

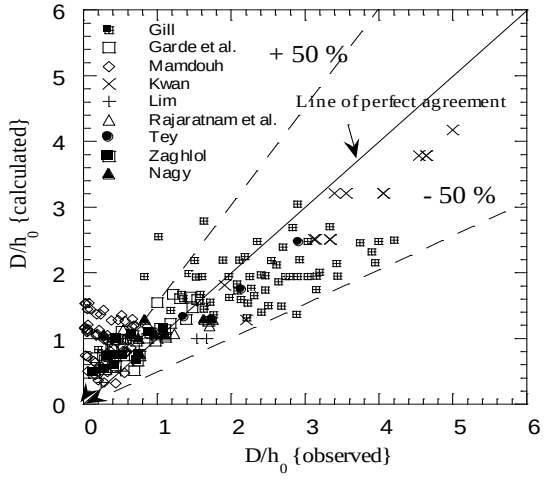


Fig. 17. Verification of Kandsamy et al. [16 ] equation.

## 12. Conclusions

Analytical and experimental analyses are presented to estimate the maximum local scour depth. It is proved theoretically and experimentally that the values of the approaching flow Froude number have significant effect on the maximum scour depth in the developed scour hole. Larger value of Froude number causes deeper scour hole. The other parameters have been shown of secondary importance. Dike length ratio and intrusion length ratio have direct proportion with the maximum scour depth ratio, while the particle size ratio is adversely proportional to the scour depth ratio. The scour hole for both repelling ( $\alpha > 90^0$) and attracting dikes ($\alpha < 90^0$) have less geometrical dimensions than the scour hole for deflecting dikes ($\alpha = 90^0$). A nonlinear regression analysis is

performed to derive an expression for calculating the maximum scour depth. The resulting values for the developed expression give much better agreement with observed data than other previous studies.

**References**


[1] M. Ahmed, "Experiments on Design and Behavior of Spur-Dikes," Proceedings of the International Hydraulic Convention, ASCE, New York, pp. 145-159 (1953).

[2] H. Liu, F. Chang, and M. Skinner, "Effect of Bridge Constriction on Scour and Backwater," Publication No. CER60HKL22, Civil Engineering Section, Colorado State University, Fort Collins, Colorado (1961).

[3] R. J. Garde, K. Subramanya and K. D. Nambudripad, "Study of Scour Around Spur-Dikes," Journal of the Hydraulic Engineering, ASCE, Vol. 87(HY. 6), pp. 23-37 (1961).

[4] E.M. Laursen, "An analysis of Relief Bridge Scour," Journal of Hydraulic Division, ASCE, Vol. 89 (3), pp. 93-118 (1963).

[5] M.A. Gill, "Erosion of Sand Beds Around Spur Dikes," Journal of the Hydraulic Engineering, ASCE, Vol. 87, (HY. 6), pp. 23-37 (1972).

[6] N. Rajaratnam and B.A. Nwachukwu, "Erosion Near Groyne-Like Structures", Journal of Hydraulic Research, Vol. 21 (4), pp. 277-287 (1983).

[7] B.W. Melville, "Local Scour at Bridge Abutments," Journal of Hydraulic Engineering, ASCE, Vol. 118 (4), pp. 615-631 (1992).

[8] B.W. Melville, "Pier and Abutment Scour: Integrated Approach," Journal of Hydraulic Engineering, ASCE, Vol. 123 (2), pp. 125-136 (1997).

[9] G. Oliveto and W.H. Hager, "Temporal Evolution of Clear-Water Pier and Abutment Scour," Journal of Hydraulic Engineering, ASCE, Vol. 128 (9), pp. 811-820 (2002).

[10] C.T. Yang, "Sediment Transport- Theory and Practice," the McGraw-Hill Series in Water Resources and Environmental Engineering (1996).

[11] N.A. Zaghloul, "Local Scour Around Spur dikes," Journal of Hydrology, Elsevier Scientific Publishing Company, 60, pp. 123-140 (1983).

[12] T.F. Kwan, "Study of Abutment Scour," Report Submitted to the Road Research Unit of the National Roads Board, University of Auckland, No. 328, New Zealand, (1984).

[13] C.B. Tey, "Local Scour at Bridge Abutments," Report Submitted to the Road Research Unit of the National Roads Board, University of Auckland, (329), New Zealand (1984).

[14] Siow-Yong Lim, "Equilibrium Clear-Water Scour Around an Abutment," Journal of the Hydraulic Engineering, ASCE, Vol. 123 (3), pp. 237-243 (1997).

[15] H.M. Mamdouh, "Scour Around Dikes," Thesis submitted in partial fulfillment for the degree of Master of Science in Civil Engineering, Alexandria University, Egypt, (2000).

[16] J.K. Kandsamy, B.W. Melville, "Maximum Local Scour Depth at Bridge Piers and Abutments," Journal of Hydraulic Research, Vol. 36 (2), pp. 183-198 (1998).


Received September 8, 2004
Accepted November 29, 2004